

ISSN: 0256-307X

中国物理快报 Chinese Physics Letters

Volume 27 Number 2 February 2010

A Series Journal of the Chinese Physical Society
Distributed by IOP Publishing

Online: <http://www.iop.org/journals/cpl>
<http://cpl.iphy.ac.cn>

CHINESE PHYSICAL SOCIETY

JUST FOR AUTHORS
— CHINESE PHYSICS LETTERS

Numerical Study on Critical Wedge Angle of Cellular Detonation Reflections *

WANG Gang(王刚)^{1,2}, ZHANG De-Liang(张德良)², LIU Kai-Xin(刘凯欣)^{1,3**}¹LTCs and College of Engineering, Peking University, Beijing 100871²LHD, Institute of Mechanics, Chinese Academy of Sciences, Beijing 100190³Center for Applied Physics and Technology, Peking University, Beijing 100871

(Received 11 February 2009)

The critical wedge angle (CWA) for the transition from regular reflection (RR) to Mach reflection (MR) of a cellular detonation wave is studied numerically by an improved space-time conservation element and solution element method together with a two-step chemical reaction model. The accuracy of that numerical way is verified by simulating cellular detonation reflections at a 19.3° wedge. The planar and cellular detonation reflections over 45° – 55° wedges are also simulated. When the cellular detonation wave is over a 50° wedge, numerical results show a new phenomenon that RR and MR occur alternately. The transition process between RR and MR is investigated with the local pressure contours. Numerical analysis shows that the cellular structure is the essential reason for the new phenomenon and the CWA of detonation reflection is not a certain angle but an angle range.

PACS: 47.40.Rs, 82.33.Vx, 02.60.Cb

DOI: 10.1088/0256-307X/27/2/024701

Detonation reflection on a wedge is a very complicated phenomenon, and it is one of the fundamental problems of detonation propagation in complex channels. Similar to the shock wave situation, regular reflection (RR) or Mach reflection (MR) occurs when a detonation wave encounters a wedge.^[1]

Studies on detonation reflections are still tentative, especially for the critical wedge angle (CWA) for the transition from RR to MR. The CWAs in different studies may be quite different even under the same research conditions. The commonest study conditions of detonation reflections are the H_2 – O_2 detonation waves whose properties are familiar to researchers. Table 1 shows the CWAs in the stoichiometric H_2 – O_2 detonation reflections. The CWAs are ranged from 32° to 83° in theoretical analysis because there is no appropriate theory for detonation reflections. The experimental results are also uncertain (39° – 50°) for the limitations of the equipment and measurement methods. Thus the numerical simulations become important in research on detonation reflections.^[2–4]

Table 1. The CWAs of H_2 – O_2 detonation waves by different means.

Researchers	Means		
	Theory analysis	Experiments	Numerical simulations
Meltzer <i>et al.</i> ^[5]	32°	40° – 45°	
Gavrilenko <i>et al.</i> ^[6]	34°	39° – 41°	
Akbar. ^[1]	33°	45° – 50°	
Li <i>et al.</i> ^[7]	42° , 83°		
Yu. ^[3]			50°
Hu <i>et al.</i> ^[4]			$\sim 48.5^\circ$

Numerical simulations of detonations have improved immensely in the recent 25 years with the development in both computational methods and avail-

able computer facilities. There are two main challenges in detonation simulations. One is the calculation of the process of energy release in the reaction flows; the other is the strategy of capturing the strong discontinuity in detonation waves. Successful solutions of the two challenges depend on the developments of chemical reaction models and numerical schemes, respectively. In this study, we adopt an improved space-time conservation element and solution element (CE/SE) scheme^[8,9] and a two-step chemical model.^[10]

The CE/SE method originally proposed by Chang^[11] in 1995 is a new numerical framework for solving conservation laws. The CE/SE method substantially differs from the existing well-established computational fluid dynamics (CFD) methods. The CE/SE method has many features such as a unified treatment of space and time, satisfying both local and global flux conservation in space and time and simple treatments under boundary conditions. Because of its simplicity, generality and accuracy, the CE/SE method has been successfully applied to fluid problems and engineering practices. However, the original two-dimensional CE/SE method^[12] is complicated by the special design of solution elements (SEs) and conservation elements (CEs). Thus, we have proposed an improved two-dimensional CE/SE scheme by adopting a general rectangle mesh to construct SEs and CEs (shown in Fig. 1)^[8] and high-order accuracy Taylor expansions.^[13] Moreover, we have extended the improved CE/SE scheme to detonation simulations and verified its accuracy.^[8,9]

Many chemical reaction models such as the C-J model, the one/two-step reaction model, Sichel's two-step reaction model and the detailed chemical reaction

*Supported by the National Natural Science Foundation of China under Grant Nos 10972010, 10732010 and 20490206.

**To whom correspondence should be addressed. Email: kliu@pku.edu.cn

© 2010 Chinese Physical Society and IOP Publishing Ltd

model have been applied to numerical simulations of detonation waves. The one/two-step chemical reaction model can describe the chemical reaction process and does not need many computing resources.^[14,15] Thus, we adopt the two-step reaction model in this study.

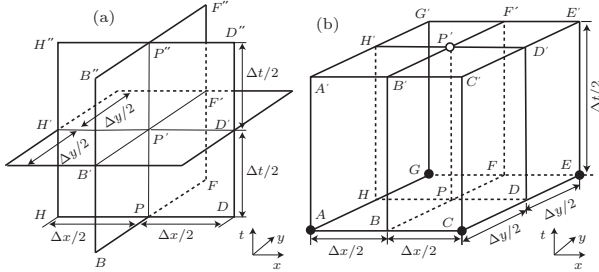


Fig. 1. Space-time geometry of the improved two-dimensional CE/SE scheme.

The two-step reaction model simplifies the complicated chemical reactions to an induction reaction and an exothermic reaction. The progress parameters α and β , for the induction reaction and the exothermic reaction, respectively, are both unity first, followed by decrease of α to zero, then β decreases until the equilibrium state is reached. The rates of α and β , ω_α and ω_β , are given as follows:^[10]

$$\omega_\alpha = \frac{d\alpha}{dt} = -k_\alpha \rho \exp\left(-\frac{E_\alpha}{RT}\right), \quad (1)$$

$$\omega_\beta = \frac{d\beta}{dt} = \begin{cases} 0, & (\alpha > 0), \\ -k_\beta p^2 \left[\beta^2 \exp\left(-\frac{E_\beta}{RT}\right) - (1 - \beta)^2 \right. \\ \left. \cdot \exp\left(-\frac{E_\beta + Q}{RT}\right) \right], & (\alpha \leq 0), \end{cases} \quad (2)$$

where ρ is the mass density, T the temperature, R the gas constant, Q the heat release parameter, k_α and k_β the constants of reaction rates, and E_α and E_β the activation energies.

The governing equations for a detonation problem are the two-dimensional Euler equations

$$\frac{\partial \mathbf{Q}}{\partial t} + \frac{\partial \mathbf{E}}{\partial x} + \frac{\partial \mathbf{F}}{\partial y} = \mathbf{S}, \quad (3)$$

where $\mathbf{Q} = (\rho, \rho u, \rho v, E, \rho\alpha, \rho\beta)^T$, $\mathbf{E} = (\rho u, \rho u^2 + p, \rho uv, (E + p)u, \rho\alpha u, \rho\beta u)^T$, $\mathbf{F} = (\rho v, \rho uv, \rho v^2 + p, (E + p)v, \rho\alpha v, \rho\beta v)^T$, $\mathbf{S} = (0, 0, 0, 0, \omega_\alpha, \omega_\beta)^T$, in which u and v are velocity components, p the pressure. E is the total energy density and defined as

$$E = \frac{p}{\gamma - 1} + \frac{\rho(u^2 + v^2)}{2} + \rho\beta Q, \quad (4)$$

where γ is the specific heat ratio.

In order to verify the accuracy of the improved CE/SE scheme and the two-step reaction model in cellular detonation reflections, we simulate a stoichiometric $\text{H}_2\text{-O}_2$ cellular detonation propagating in a channel

with a 19.3° wedge. The initial pressure and temperature are 1 atm and 298 K, respectively. The ignition condition of pressure in the channel left is 40 atm. The computing parameters of the two-step reaction model for the stoichiometric $\text{H}_2\text{-O}_2$ gas mixture are given as $Q = 1.33 \times 10^7 \text{ J/kg}$, $k_\alpha = 3.0 \times 10^8 \text{ m}^3/\text{kg/s}$, $k_\beta = 1.875 \times 10^{-5} \text{ m}^4/\text{N}^2/\text{s}$, $E_\alpha = 2.261 \times 10^7 \text{ J/kg}$, $E_\beta = 4.6151 \times 10^6 \text{ J/kg}$.^[10]

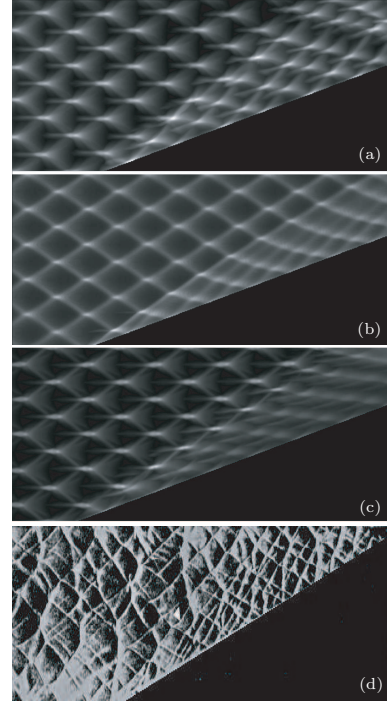


Fig. 2. Cellular patterns of detonation waves over the 19.3° wedge: (a) Numerical simulation (400×200 meshes), (b) Sichel's two-step reaction model (400×200 meshes), (c) detailed chemical reaction model (400×200 meshes), (d) experiment of Guo *et al.* in 2001.

Figure 2 shows the cellular patterns by the numerical simulation (using the two-step reaction model, Sichel's two-step reaction model^[16] and the detailed chemical reaction model^[17] respectively) and the corresponding experiment.^[18] The numerical cellular patterns by the three chemical reaction models all can obtain clear cellular structure and can describe the basic phenomena of the cellular detonation reflection, e.g., the triple-point trajectory is not a straight line and the cell sizes between the triple-point trajectory and the wedge become smaller. Table 2 shows the characteristic parameters of cellular patterns and detonation reflections under different computing meshes and different chemical reaction models. We can find that the numerical parameters by the two-step reaction model can agree well with the experimental ones at the five mesh types. The numerical parameters by Sichel's two-step reaction model and the detailed chemical reaction model can also agree well with the experimental ones, but they cost more computing resources, such as memory ($M_{\text{two-step}} : M_{\text{Sichel's}} : M_{\text{detailed}} = 1.0 : 1.4 : 3.1$)

and computing time ($t_{\text{two-step}} : t_{\text{Sichel's}} : t_{\text{detailed}} = 1.0 : 2.5 : 3.2$).

Table 2. Characteristic parameters of cellular patterns and detonation reflections. Here a is the ratio of cell width to cell length, ϕ is the exit angle, χ is the entrance angle, ψ is the angle of the transverse wave trace, ξ is the angle between the triple-point trajectory and the wedge.

	a	ϕ (deg)	χ (deg)	ψ (deg)	ξ (deg)	Meshes
Experiment	0.5–0.6	5–10	32–40	~ 30	11.5–13.0	
Two-step	0.59	9.2	38.0	30.5	~ 13.1	400×200
Two-step	0.56	9.0	36.2	29.24	~ 13.0	600×300
Two-step	0.53	8.5	33.3	29.12	~ 12.9	800×400
Two-step	0.53	8.5	33.2	29.10	~ 12.9	1000×500
Two-step	0.53	8.5	33.2	29.08	~ 12.9	1200×600
Sichel's	0.60	11.2	31.5	29.0	~ 11.3	400×200
Detailed	0.51	9.5	38.2	28.5	~ 12.2	400×200

We simulate the planar and cellular detonation reflections at different wedge angles (ranging from 45° to 55° with 0.5° interval). The grid sizes are 1200×750 and the CFL number equals 0.5. Similar to reflections of shock waves,^[19] the reflection of planar detonation is a self-similar phenomenon. The CWA of the planar detonation is 49.5° . However, the reflection of cellular detonation is not a self-similar phenomenon for the complex wave system in the detonation front. Summarizing the numerical results of cellular detonation reflections, we can find the following phenomena: (1) MR occurs when the cellular detonations are over the wedges whose angles are less than 49.5° . (2) RR occurs when the cellular detonations are over the wedges whose angles are greater than 50.5° . (3) RR and MR occur alternately when the cellular detonation wave is over the 50° wedge.

The phenomenon of RR and MR occurring alternately under steady environment conditions (a steady detonation wave and a wedge with fixed angle) does not occur in the shock wave reflections. That phe-

nomenon has not been observed because of the limitations of the measurement equipment and methods. In this study, we describe and analyze the phenomenon by the numerical results.

Figure 3 shows the transition process from RR to MR of the cellular detonation over the 50° wedge by describing the local pressure contours every 20 steps between steps 2800 ($56.65 \mu\text{s}$) and 3860 ($60.88 \mu\text{s}$). In order to distinguish the Mach stem in the precursor shock wave (see step 2800), we call the Mach stem between the wedge and the precursor shock wave the MSWP (see step 2860). At step 2800, RR occurs because there is no MSWP, though the wave system behind the detonation front is complex. We can also find that one transverse wave has collided with the wedge and that enhances the pressure between the wedge and the reflection wave of the detonation wave. The reflected wave of the transverse wave also begins to interact with the reflected wave of the detonation wave. Both the facets strengthen the reflected wave of the detonation wave. Thus at step 2820 a MSWP begin to form at the detonation front near the wedge. At step 2840 we can find the MSWP near the wedge. At step 2860 the MSWP can be distinguished more clearly.

Figure 4 shows the transition process from MR to RR. MR occurs between steps 2960 ($62.76 \mu\text{s}$) and 3020 ($64.04 \mu\text{s}$). At step 2980 the transverse wave interacts with the reflected wave of the detonation wave and that also weakens the reflection wave of the detonation wave. At step 3000 the MSWP disappears before the reflection wave of the transverse wave interacts with the reflection wave of the detonation wave. At step 3200 RR occurs though the reflection wave of the transverse wave has interacted with the reflection wave of the detonation wave. The numerical results show the transition cycle time is about $4 \mu\text{s}$.

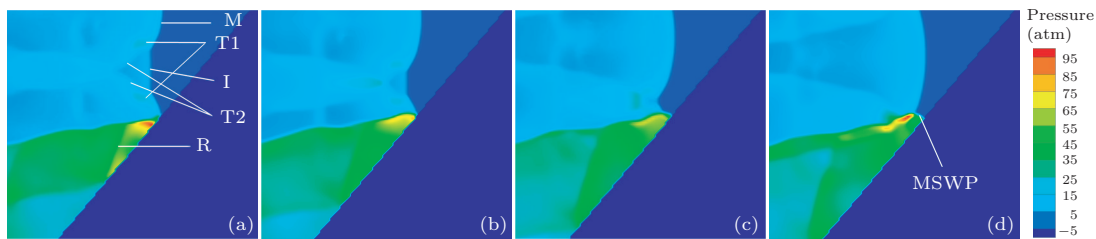


Fig. 3. Local pressure contours every 20 steps between steps 2800 and 2860 (M: Mach stem in the precursor shock wave, I: incident wave, T1: triple points, T2: transverse wave, R: reflected wave of transverse wave, MSWP: Mach stem between the wedge and the precursor shock wave).

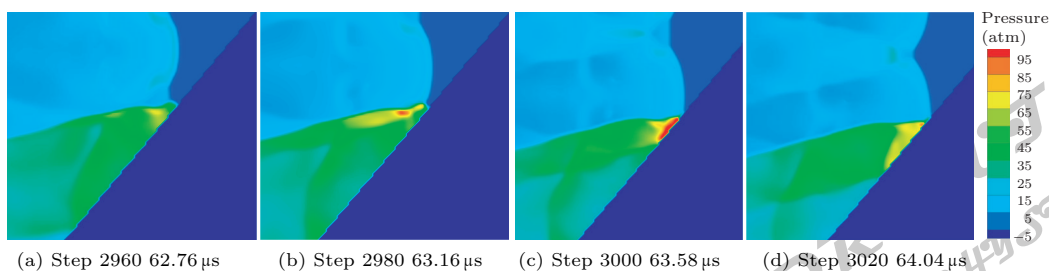


Fig. 4. Local pressure contours every 20 steps between steps 2960 and 3020.

Figure 5 shows that the velocity profiles of planar and cellular detonation waves at different times. The maximum particle velocities in the planar detonation front keep the same value (1910 ± 10 m/s) at different times. The self-similar distribution of physical quantities is the reason for the self-similar phenomena of planar detonation reflections. The maximum particle velocities in the cellular detonation front range from 1387.5 m/s to 2415.6 m/s at different times. The sound velocity in the initial $\text{H}_2\text{-O}_2$ gas mixture is 536.6 m/s. Thus the Mach numbers in the planar and cellular detonation fronts are 3.56 and 2.59–4.50, respectively. From the theory of shock wave^[19] and planar detonation^[7] reflections we know that the reflection types are decided by the Mach number if the wedge angle is fixed. Akbar's experiments^[1] also show that reflection types of the detonation wave and shock wave have the same trend, though the detonation waves and shock waves have different waveforms. For planar detonation waves, the CWA is 49.5° in our study. This means that RR will occur if the Mach number is less than 3.56, and MR will occur if the Mach number is greater than 3.56 when the detonation wave encounters the 49.5° wedge. The Mach number of the cellular detonation wave ranges from 2.59 to 4.50, so RR and MR can occur alternately in the same wedge.

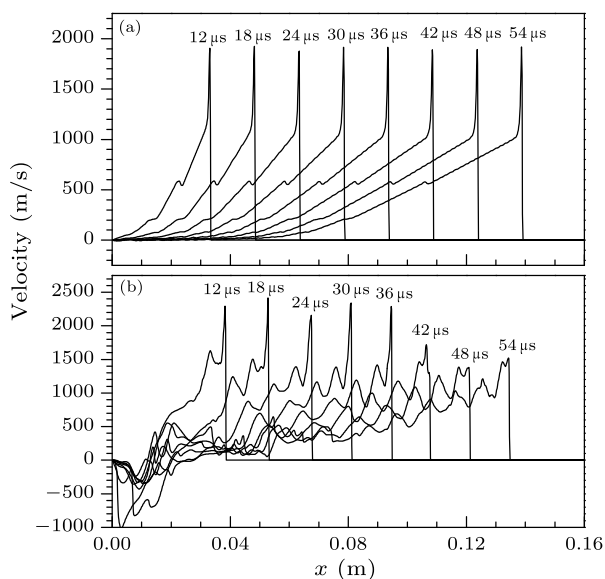


Fig. 5. Velocity profiles at different times: (a) planar detonation wave, (b) cellular detonation wave.

From the description we can find that the transverse waves play an important role in the transition process between RR and MR. From the analysis we know that the non-self-similarity of physical quantities is the reason for RR and MR occurring alternately. The mechanism of cellular structure is still a disputed problem, though some researchers thought that the transverse waves are the key character of cel-

lular detonations.^[20] However, it is widely accepted that the cellular structure is an inherent characteristic of detonation waves. Thus we believe that RR and MR can occur alternately with a steady detonation over a wedge with an appropriate angle and the CWA of detonation reflections is not a certain angle but an angle range.

In conclusion, the improved CE/SE scheme and the two-step chemical model have been introduced and verified for studying the CWA of cellular detonation reflections. We find that RR and MR occur alternately when the stoichiometric $\text{H}_2\text{-O}_2$ cellular detonation wave encounters the 50° wedge. The phenomenon of RR and MR occurring at the same wedge is essentially different from the reflections of planar detonation waves and shock waves. We describe the transition process between RR and MR aided by the local pressure contours. We analyze the reason for RR and MR occurring alternately using the numerical data and the theory of planar detonation reflections. The results show that the cellular structure of detonation waves induces the new phenomenon and the CWA of detonation reflection is not a certain angle but an angle range.

The CWA of the stoichiometric $\text{H}_2\text{-O}_2$ cellular and planar detonation reflection is $49.5^\circ\text{--}50.5^\circ$ and 49.5° , respectively. The CWA of the planar detonation reflection, which is approximately equal to that of the cellular detonation reflection, can be used in engineering designs.

References

- [1] Akbar R 1997 *PhD Dissertation* (Rensselaer Polytechnic Institute)
- [2] Ohya S et al 2000 *Shock Waves* **10** 185
- [3] Yu Q 1996 *PhD Dissertation* (RWTH, Aachen, Germany)
- [4] Hu Z M et al 2004 *Acta Mech. Sin.* **36** 385
- [5] Meltzer J et al 1991 *Progress in Astronautics and Aeronautics* **153** 78
- [6] Gavrilenko T P and Prokhorov E S 1982 *Combust. Explor. Shock* **17** 689
- [7] Li H, Ben-Dor G and Gronig H 1997 *AIAA J.* **35** 1712
- [8] Wang G, Zhang D L and Liu K X 2007 *Chin. Phys. Lett.* **24** 3563
- [9] Wang G et al 2010 *Comput. Fluids* **39** 168
- [10] Taki S and Fujiwara T 1984 *Progress in Astronautics and Aeronautics* **94** 186
- [11] Chang S C 1995 *J. Comput. Phys.* **119** 295
- [12] Chang S C, Wang X Y and Chow C Y 1999 *J. Comput. Phys.* **156** 89
- [13] Liu K X and Wang J T 2004 *Chin. Phys. Lett.* **21** 2085
- [14] Wang C, Jiang Z L and Gao Y L 2008 *Chin. Phys. Lett.* **25** 3704
- [15] Han G L et al 2008 *Chin. Phys. Lett.* **25** 2125
- [16] Sichel M et al 2002 *Proc. R. Soc. London A* **458** 49
- [17] Kee R J et al 1996 *SAND96-8216*
- [18] Guo C M, Zhang D L and Xie W 2001 *Combust. Flame* **127** 2051
- [19] Ben-Dor G 1978 *UTIAS Repotr No 232*
- [20] Kailasanath K et al 1985 *Combust. Flame* **61** 199

Chinese Physics Letters

Volume 27

Number 2

2010

GENERAL

- 020201 Exact Solutions for Two Equation Hierarchies**
ZHAO Song-Lin, ZHANG Da-Jun, JI Jie
- 020202 Lie Point Symmetries and Exact Solutions of the Coupled Volterra System**
LIU Ping, LOU Sen-Yue
- 020301 Realizing the Underlying Quantum Dynamical Algebra $SU(2)$ in Morse Potential**
WANG Xue-Hong, LIU Yu-Bin
- 020302 Universal Quantum Cloning Machine in Circuit Quantum Electrodynamics**
LV Dan-Dan, LU Hong, YU Ya-Fei, FENG Xun-Li, ZHANG Zhi-Ming
- 020401 Statistical Mechanical Entropy of a $(4 + n)$ -Dimensional Static Spherically Symmetric Black Hole**
ZHAO Fan, HE Feng
- 020402 Cosmological Gravitational Wave in de Sitter Spacetime**
LIU Liao
- 020501 Fuzzy Modeling and Impulsive Control of a Memristor-Based Chaotic System**
ZHONG Qi-Shui, YU Yong-Bin, YU Jue-Bang
- 020502 Synchronization Control of Two Different Chaotic Systems with Known and Unknown Parameters**
GUAN Jun-Biao
- 020503 Noise Effects on Temperature Encoding of Neuronal Spike Trains in a Cold Receptor**
DU Ying, LU Qi-Shao
- 020504 Analysis of Chaotic Dynamics in a Two-Dimensional Sine Square Map**
XU Jie, LONG Ke-Ping, FOURNIER-PRUNARET Danièle, TAHA Abdel-Kaddous, CHARGE Pascal
- 020505 Periodic, Quasiperiodic and Chaotic q -Breathers in a Fermi-Pasta-Ulam Lattice**
XU Quan, TIAN Qiang
- 020506 Spinless Bosons in a 1D Harmonic Trap with Repulsive Delta Function Interparticle Interaction II: Numerical Solutions**
MA Zhong-Qi, C. N. Yang
- 020507 Spectrum Analysis and Circuit Implementation of a New 3D Chaotic System with Novel Chaotic Attractors**
DONG Gao-Gao, ZHENG Song, TIAN Li-Xin, DU Rui-Jin
- 020508 A Scheme for Information Erasure in a Double-Well Potential**
WANG Xin-Xin, BAO Jing-Dong

THE PHYSICS OF ELEMENTARY PARTICLES AND FIELDS

- 021101 Transition Temperature of Lattice Quantum Chromodynamics with Two Flavors with a Small Chemical Potential**
WU Liang-Kai

NUCLEAR PHYSICS

- 022101 Lifetimes of High Spin States in an Odd-Proton Nucleus ^{129}Cs**
WANG Lie-Lin, ZHU Li-Hua, LU Jing-Bin, WU Xiao-Guang, LI Guang-Sheng, HAO Xin, ZHENG Yun, HE Chuang-Ye, WANG Lei, LI Xue-Qin, LIU Ying, PAN Bo, ZHAO Yan-Xin, LI Zhong-Yu, DING Huai-Bo
- 022102 Nuclear Structure and Magnetic Moment of the Unstable ^{12}B – ^{12}N Mirror Pair**
ZHENG Yong-Nan, ZHOU Dong-Mei, YUAN Da-Qing, ZUO Yi, FAN Ping, M. Mihara, K. Matsuta, M. Fukuda, T. Suzuki, XU Yong-Jun, ZHU Jia-Zheng, WANG Zhi-Qiang, LUO Hai-Long, ZHANG Sheng-Yun

(Continued on inside back cover)

- 022103 Clustering Structure of ^{10}Be Studied with the Deformed RMF+BCS Method**
ZHONG Ming-Fei, LI Jia-Xing, ZHANG Deng-Gao, HAN Rui, JI Juan-Xia, CHEN Li-Xiang
- 022301 Observation of a Possible New Isomer in ^{175}Ir**
WANG Hua-Lei, SONG Li-Tao, ZHAO Wei-Juan, LIU Zhong-Xia, ZHANG Yu-Hu, ZHOU Xiao-Hong, GUO Ying-Xiang, LEI Xiang-Guo
- 022501 Interferometry Signatures for QCD First-Order Phase Transition in High Energy Heavy Ion Collisions**
YU Li-Li, M. J. Efaaf, ZHANG Wei-Ning
- ATOMIC AND MOLECULAR PHYSICS**
- 023201 Dynamics of a Rydberg Hydrogen Atom in a Generalized van der Waals Potential and a Magnetic Field**
WANG De-Hua
- 023202 Elastic Scattering of Ultracold ^{23}Na and ^{39}K Atoms in the Singlet State**
HU Qiu-Bo, ZHANG Yong-Sheng, SUN Jin-Feng
- 023701 Continuous Imaging of a Single Neutral Atom in a Variant Magneto-Optical Trap**
XIA Tian, ZHOU Shu-Yu, CHEN Peng, LI Lin, HONG Tao, WANG Yu-Zhu
- FUNDAMENTAL AREAS OF PHENOMENOLOGY(INCLUDING APPLICATIONS)**
- 024201 High Efficiency Multi-kW Diode-Side-Pumped Nd:YAG Laser with Reduced Thermal Effect**
XU Yi-Ting, XU Jia-Lin, CUI Qian-Jin, XIE Shi-Yong, LU Yuan-Fu, BO Yong, PENG Qin-Jun, CUI Da-Fu, XU Zu-Yan
- 024202 Characterizations of Stress and Strain Variation in Three-Dimensional Forming of Laser Micro-Manufacturing**
ZHOU Ming, ZHAO Guo-Huan, HUANG Tao, DING Hua, CAI Lan
- 024203 Self-Collimation in Planar Photonic Crystals Fabricated by CMOS Technology**
YANG Zhi-Feng, WU Ai-Min, FANG Na, JIANG Xun-Ya, LIN Xu-Lin, WANG Xi, ZOU Shi-Chang
- 024204 Photoinduced Reorientation Process and Nonlinear Optical Properties of Ag Nanoparticle Doped Azo Polymer Films**
DENG Yan, SHEN Jing
- 024205 A Transverse-Longitudinal Cross-Spectral Density Matrix of Partially Coherent Electromagnetic Beams**
LI Jian-Long, TANG Shi-Hong, LU Bai-Da
- 024206 A Single-Fundamental-Mode Photonic Crystal Vertical Cavity Surface Emitting Laser**
XIE Yi-Yang, XU Qiang, WANG Chun-Xia, LIU Ying-Ming, WANG Bao-Qiang, CHEN Hong-Da, SHEN Guang-Di
- 024207 Theoretical Studies of Optical Properties of Silver Nanoparticles**
MA Ye-Wan, WU Zhao-Wang, ZHANG Li-Hua, ZHANG Jie
- 024208 Micro Extrinsic Fiber-Optic Fabry–Perot Interferometric Sensor Based on Erbium- and Boron-Doped Fibers**
RAO Bing, RAN Zeng-Ling, GONG Yuan
- 024209 Double-Arched LD Array Stagger Pumped Electro-Optic Q-Switched Nd:YAG Laser without Water Cooling**
CHEN Xin-Yu, JIN Guang-Yong, YU Yong-Ji, WANG Chao, HAO Da-Wei, WANG Yi-Bo
- 024210 Wavelet-Transform Spectrum for Quantum Optical States**
SONG Jun, FAN Hong-Yi
- 024211 An Efficient Pulsed CH_3OH Terahertz Laser Pumped by a TEA CO_2 Laser**
JIU Zhi-Xian, ZUO Du-Luo, MIAO Liang, QI Chun-Chao, CHENG Zu-Hai
- 024212 High Current Operation of a Semi-insulating Gallium Arsenide Photoconductive Semiconductor Switch Triggering a Spark Gap**
XU Ming, SHI Wei, HOU Lei, XUE Hong, WU Shen-Jiang, DAI Hui-Ying

- 024213 Slow Light Effect and Multimode Lasing in a Photonic Crystal Waveguide Microlaser**
XING Ming-Xin, ZHENG Wan-Hua, ZHOU Wen-Jun, CHEN Wei, LIU An-Jin, WANG Hai-Ling
- 024214 Design of a Fused-Silica Subwavelength Polarizing Beam Splitter Grating Based on the Modal Method**
ZHAO Hua-Jun, YUAN Dai-Rong, WANG Pei, LU Yong-Hua, MING Hai
- 024215 Accurate Phase Shift Extraction for Generalized Phase-Shifting Interferometry**
XU Xian-Feng, CAI Lu-Zhong, WANG Yu-Rong, LI Dai-Lin
- 024216 Effect of Air Gap on Dual-Tripler Broadband Third-Harmonic Generation**
HAN Wei, WANG Fang, WANG Li-Quan, JIA Huai-Ting, WANG Wei, LI Fu-Quan, FENG Bin, XIANG Yong, LI Ke-Yu, ZHONG Wei
- 024401 Flow Reversal of Fully-Developed Mixed MHD Convection in Vertical Channels**
H. Saleh, I. Hashim
- 024701 Numerical Study on Critical Wedge Angle of Cellular Detonation Reflections**
WANG Gang, ZHANG De-Liang, LIU Kai-Xin
- 024702 Key Factors in Determining the Magnitude of Vorticity in Turbulent Plane Wakes**
MI Jian-Chun, R. A. Antonia
- 024703 Stretching a Curved Surface in a Viscous Fluid**
M. Ali, T. Javed, Z. Abbas
- 024704 Static Threshold Pressure Gradient Characteristics of Liquid Influenced by Boundary Wettability**
SONG Fu-Quan, WANG Jian-Dong, LIU Hai-Li
- 024705 Fractal Analysis of Surface Roughness of Particles in Porous Media**
CAI Jian-Chao, YU Bo-Ming, ZOU Ming-Qing, MEI Mao-Fei
- 024706 Late-Stage Vortical Structures and Eddy Motions in a Transitional Boundary Layer**
LIU Xiao-Bing, CHEN Zheng-Qing, LIU Chao-Qun
- 024707 Three-Dimensional Linear Instability Analysis of Thermocapillary Return Flow on a Porous Plane**
ZHAO Si-Cheng, LIU Qiu-Sheng, NGUYEN-THI Henri, BILLIA Bernard
- 024708 Lagrangian Structure Function's Scaling Exponents in Turbulent Channel Flow**
LUO Jian-Ping, LU Zhi-Ming, USHIJIMA Tatsuo, KITOH Osami, LIU Yu-Lu
- PHYSICS OF GASES, PLASMAS, AND ELECTRIC DISCHARGES**
- 025201 Particle Simulation of Electrostatic Waves Driven by an Electron Beam**
GUO Jun
- 025202 Numerical Simulation of Anisotropic Preheating Ablative Rayleigh–Taylor Instability**
WANG Li-Feng, YE Wen-Hua, LI Ying-Jun
- 025203 Two-Dimensional Rayleigh–Taylor Instability in Incompressible Fluids at Arbitrary Atwood Numbers**
WANG Li-Feng, YE Wen-Hua, LI Ying-Jun
- 025204 Lattice Waves in Two-Dimensional Hexagonal Quantum Plasma Crystals**
SUN Xiao-Xia, WANG Chun-Hua, GAO Feng
- 025205 Surface Wave Analysis of Planar-Type Overdense Plasma with Surface Plasmon Polariton Resonance**
CHEN Zhao-Quan, LIU Ming-Hai, TANG Liang, LV Jian-Hong, HU Xi-Wei
- CONDENSED MATTER: STRUCTURE, MECHANICAL AND THERMAL PROPERTIES**
- 026101 Mechanical Properties and Anisotropy in PBWO_4 Single Crystal**
WANG Hong, ZHANG Zhi-Jun, ZHAO Jing-Tai, XU Jia-Yue, HU Guan-Qin, LI Pei-Jun
- 026102 Superconducting State Parameters of $\text{Nb}_x\text{Ta}_y\text{Mo}_z$ Superconductors**
Aditya M. Vora

- 026103 Raman Investigation of Sodium Titanate Nanotubes under Hydrostatic Pressures up to 26.9 GPa**
TIAN Bao-Li, DU Zu-Liang, MA Yan-Mei, LI Xue-Fei, CUI Qi-Liang, CUI Tian, LIU Bing-Bing, ZOU Guang-Tian
- 026104 Mechanical Behavior of Nanometer Ni by Simulating Nanoindentation**
TANG Qi-Heng, YANG Tian-Yong, DING Lan
- 026105 Formability and Thermal Stability of $\text{Ce}_{62}\text{Al}_{15}\text{Fe}_8\text{Co}_{15}$ Bulk Metallic Glass**
WANG Zhi-Xin, LU Jin-Bin, YANG Wei-Tie
- 026201 Comparison Study on Characteristic Regimes in Shocked Porous Materials**
XU Ai-Guo, ZHANG Guang-Cai, LI Hua, ZHU Jian-Shi
- 026401 Metastable Phase Separation and Concomitant Solute Redistribution of Liquid Fe-Cu-Sn Ternary Alloy**
ZHANG Xiao-Mei, WANG Wei-Li, RUAN Ying, WEI Bing-Bo
- 026501 Molecular Dynamics Simulation of Strontium Titanate**
SEETAWAN Tosawat, WONG-UD-DEE Gjindara, THANACHAYANONT Chanchana, AMORNKITBUMRUNG Vittaya
- 026502 Thermal Depth Profiling Reconstruction by Multilayer Thermal Quadrupole Modeling and Particle Swarm Optimization**
CHEN Zhao-Jiang, ZHANG Shu-Yi
- 026801 Self-Assembly of TBrPP-Co Molecules on an Ag/Si(111) Surface Studied by Scanning Tunneling Microscopy**
LI Qing, Shiro Yamazaki, Toyooki Eguchi, MA Xu-Cun, JIA Jin-Feng, XUE Qi-Kun, Yukio Hasegawa
- 026802 Atomic-Scale Study of Ge-Induced Incommensurate Phases on Si(111)**
WU Rui, WANG Li-Li, ZHANG Yi, MA Xu-Cun, JIA Jin-Feng, XUE Qi-Kun
- 026803 Aggregation Behavior of Metal-Ethylene Complexes and Its Effect on Hydrogen Storage Capacity**
WANG Xiao-Xiong, LI Hong-Nian, YAO Chang-Hong
- 026804 Effects of Rapid Thermal Processing on Microstructure and Optical Properties of As-Deposited Ag_2O Films by Direct-Current Reactive Magnetron Sputtering**
GAO Xiao-Yong, FENG Hong-Liang, ZHANG Zeng-Yuan, MA Jiao-Min, LU Jing-Xiao
- CONDENSED MATTER: ELECTRONIC STRUCTURE, ELECTRICAL, MAGNETIC, AND OPTICAL PROPERTIES**
- 027101 Mechanical and Magnetic Properties of Rh and RhH: First-Principles Calculations**
CUI Xin, WANG Jian-Tao, LIANG Xi-Xia, ZHAO Guo-Zhong
- 027102 Degradation of AlGaIn/GaN High Electron Mobility Transistors with Different AlGaIn Layer Thicknesses under Strong Electric Field**
YANG Ling, MA Jing-Jing, ZHU Cheng, HAO Yue, MA Xiao-Hua
- 027201 Second Harmonic Detection of Spin-Dependent Transport in Magnetic Nanostructures**
YU Hai-Ming, S. Granville, YU Da-Peng, J-Ph. Ansermet
- 027202 Ultraviolet Sensitive Ultrafast Photovoltaic Effect in Tilted KTaO_3 Single Crystals**
XING Jie, GUO Er-Jia, JIN Kui-Juan, LU Hui-Bin, HE Meng, WEN Juan, YANG Fang
- 027203 Competition between Radiative Power and Dissipation Power in the Refrigeration Process in Oxide Multifilms**
ZHANG Li-Li, HU Chun-Lian, WANG Can, LÜ Hui-Bin, HAN Peng, YANG Guo-Zhen, JIN Kui-Juan
- 027301 Clockwise vs Counter-Clockwise $I-V$ Hysteresis of Point-Contact Metal-Tip/ $\text{Pr}_{0.7}\text{Ca}_{0.3}\text{MnO}_3$ /Pt Devices**
GANG Jian-Lei, LI Song-Lin, LIAO Zhao-Liang, MENG Yang, LIANG Xue-Jin, CHEN Dong-Min
- 027302 Low-Cost UV-IR Dual Band Detector Using Nonporous ZnO Film Sensitized by PbS Quantum Dots**
SHAO Jia-Feng, A. G. U. Perera, P. V. V. Jayaweera, HE De-Yan
- 027303 Bending Loss Calculation of a Dielectric-Loaded Surface Plasmon Polariton Waveguide Structure**
YUE Song, LI Jian-Jun, GONG Qi-Huang

- 027304 Effects of End Termination on Electronic Transport in a Molecular Switch**
ZHAO Peng, ZHANG Zhong, WANG Pei-Ji, ZHANG Hai-Kui, REN Miao-Juan, LI Feng
- 027701 Preparation of Ultra Low- k Porous SiOCH Films from Ring-Type Siloxane with Unsaturated Hydrocarbon Side Chains by Spin-On Deposition**
YANG Chun-Xiao, ZHANG Chi, SUN Qing-Qing, XU Sai-Sheng, ZHANG Li-Feng, SHI Yu, DING Shi-Jin, ZHANG Wei
- 027702 Microwave Absorbing Materials: Solutions for Real Functions under Ideal Conditions of Microwave Absorption**
HUANG Yao-Qing, YUAN Jie, SONG Wei-Li, WEN Bo, FANG Xiao-Yong, CAO Mao-Sheng
- 027703 Influence of Radio-Frequency Power on Structural and Electrical Properties of Sputtered Hafnium Dioxide Thin Films**
LIU Wen-Ting, LIU Zheng-Tang, TAN Ting-Ting, YAN Feng
- 027704 Effects of Substitution of Sm for Bi in BiFeO₃ Thin Films Prepared by the Sol-Gel Method**
HUANG Ning-Xiang, ZHAO Li-Feng, XU Jia-Yang, CHEN Ji-Li, ZHAO Ji-Li, ZHAO Yong
- 027801 High Characteristic Temperature 1.3 μ m InAs/GaAs Quantum-Dot Lasers Grown by Molecular Beam Epitaxy**
JI Hai-Ming, YANG Tao, CAO Yu-Lian, XU Peng-Fei, GU Yong-Xian, MA Wen-Quan, WANG Zhan-Guo
- 027802 Irradiation Effects of Femtosecond Pulses on Refractive Index of Ag-Embedded Nanocomposite Glasses**
DONG Zhi-Wei, QIAN Shi-Xiong, YANG Xiu-Chun, CHEN De-Ying
- CROSS-DISCIPLINARY PHYSICS AND RELATED AREAS OF SCIENCE AND TECHNOLOGY**
- 028101 CuInSe₂ Films Prepared by a Plasma-Assisted Selenization Process in Different Working Pressures**
YU Tao, ZHANG Yi, LI Bao-Zhang, JIANG Wei-Long, WANG He, CAI Yong-An, LIU Wei, LI Feng-Yan, SUN Yun
- 028401 Nanoscale Tapered Pt Bottom Electrode Fabricated by FIB for Low Power and Highly Stable Operations of Phase Change Memory**
LV Shi-Long, SONG Zhi-Tang, LIU Yan, FENG Song-Lin
- 028501 Design and Characterization of Evanescently Coupled Uni-Traveling Carrier Photodiodes with a Multimode Diluted Waveguide Structure**
ZHANG Yun-Xiao, PAN Jiao-Qing, ZHAO Ling-Juan, ZHU Hong-Liang, WANG Wei
- 028502 Electrical Response of Flexible Vanadyl-Phthalocyanine Thin-Film Transistors under Bending Conditions**
WANG He, LI Chun-Hong, WANG Li-Juan, WANG Hai-Bo, YAN Dong-Hang
- 028503 Electromechanical Behavior of Interdigitated SiO₂ Cantilever Arrays**
GUAN Zhi-Qiang, LUO Gang, MONTELIUS Lars, XU Hong-Xing
- 028701 Effects of CRAC Channel on Spatiotemporal Ca²⁺ Patterns in T Cells**
LI Cong-Xin, CHEN Xiao-Fang, WANG Peng-Ye, WANG Wei-Chi
- 028702 Emergent Travelling Pattern in a Spatial Predator-Prey System**
LIU Pan-Ping
- 028703 Stability of Novel Time-Sharing Dual Optical Tweezers Using a Rotating Tilt Glass Plate**
REN Yu-Xuan, WU Jian-Guang, CHEN Man, LI Huang, LI Yin-Mei
- 028704 Coarse-Grained Molecular Dynamics Simulation of a Red Blood Cell**
JIANG Li-Guo, WU Heng-An, ZHOU Xiao-Zhou, WANG Xiu-Xi
- 028901 Condensation of Self-Driven Particles in Scale-Free Networks**
SHEN Jing
- GEOPHYSICS, ASTRONOMY, AND ASTROPHYSICS**
- 029401 Is the Near-Earth Current Sheet Prior to Reconnection Unstable to Tearing Mode?**
WEI Xin-Hua, CAO Jin-Bin, ZHOU Guo-Cheng, FU Hui-Shan
- 029701 Timing and Spectral Studies of Pulsar EXO2030+375**
Shubhra Tiwari, S. N. A. Jaaffrey, Rizwan S. Khan, Sushil K. Gandhi, Santvana Bapna